FEMS Microbiology Letters, 364, 2017, fnx195

doi: 10.1093/femsle/fnx195
Advance Access Publication Date: 12 September 2017
Research Letter

RESEARCH LETTER – Physiology & Biochemistry

HU content and dynamics in *Escherichia coli* during the cell cycle and at different growth rates

Anteneh Hailu Abebe[1,2], Alexander Aranovich[1] and Itzhak Fishov[1,*]

[1]Department of Life Sciences, Ben-Gurion University of the Negev, PO Box 653, Beer-Sheva 8410501, Israel and [2]Medical Biotechnology Unit, Institute of Biotechnology, Addis Ababa University, PO Box 1176, Addis Ababa, Ethiopia

*Corresponding author: Department of Life Sciences, Ben-Gurion University of the Negev, PO Box 653, Beer-Sheva 8410501, Israel. Tel: +972-8-646-1368; Fax: +972-8-646-1710; E-mail: fishov@bgu.ac.il

One sentence summary: The concentration of histone-like HU protein in *Escherichia coli* is maintained constant throughout the cell cycle, whereas it increases in a growth rate-dependent manner, resulting in a higher HU/DNA stoichiometry.

Editor: Sylvie Rimsky

ABSTRACT

DNA-binding proteins play an important role in maintaining bacterial chromosome structure and functions. Heat-unstable (HU) histone-like protein is one of the most abundant of these proteins and participates in all major chromosome-related activities. Owing to its low sequence specificity, HU fusions with fluorescent proteins were used for general staining of the nucleoid, aiming to reveal its morphology and dynamics. We have exploited a single chromosomal copy of *hupA-egfp* fusion under the native promoter and used quantitative microscopy imaging to investigate the amount and dynamics of HUα in *Escherichia coli* cells. We found that in steady-state growing populations the cellular HUα content is proportional to the cell size, whereas its concentration is size independent. Single-cell live microscopy imaging confirmed that the amount of HUα exponentially increases during the cell cycle, but its concentration is maintained constant. This supports the existence of an auto-regulatory mechanism underlying the HUα cellular level, in addition to reflecting the gene copy number. Both the HUα amount and concentration strongly increase with the cell growth rate in different culture media. Unexpectedly, the HU/DNA stoichiometry also remarkably increases with the growth rate. This last finding may be attributed to a higher requirement for maintaining the chromosome structure in nucleoids with higher complexity.

Keywords: histone-like protein HU; *hup-egfp*; cell growth rate; nucleoid complexity; bacterial cell cycle; *Escherichia coli*

INTRODUCTION

The bacterial chromosome is highly compacted within the nucleoid body and its morphology is shaped by several factors, in particular, by different DNA-binding proteins (Dillon and Dorman 2010). Heat-unstable (HU) protein is one of the most abundant nucleoid-associated proteins in the bacterial cell. It is a small, basic, HU DNA-binding protein (Bahloul, Boubrik and Rouviere-Yaniv 2001), known to have a low sequence specificity (Becker, Kahn and Maher 2008; Dillon and Dorman 2010; Wei *et al.* 2014). The major structural roles of HU are DNA bending (Hodges-Garcia, Hagerman and Pettijohn 1989; Aki and Adhya 1997; van Noort *et al.* 2004) and constraining negative supercoils (Broyles and Pettijohn 1986; Dame and Goosen 2002). It also participates in all DNA-dependent functions, including replication, repair, recombination and gene regulation (Kamashev and Rouviere-Yaniv 2000; Dorman and Deighan 2003). Specifically, it also plays a role in regulating the initiation process of DNA replication (Bahloul, Boubrik and Rouviere-Yaniv 2001; Chodavarapu *et al.* 2008). Its interaction networks can promote nucleoid reorganization and transcriptional regulation (Berger *et al.* 2010; Hammel *et al.* 2016).

Received: 8 May 2017; **Accepted:** 11 September 2017

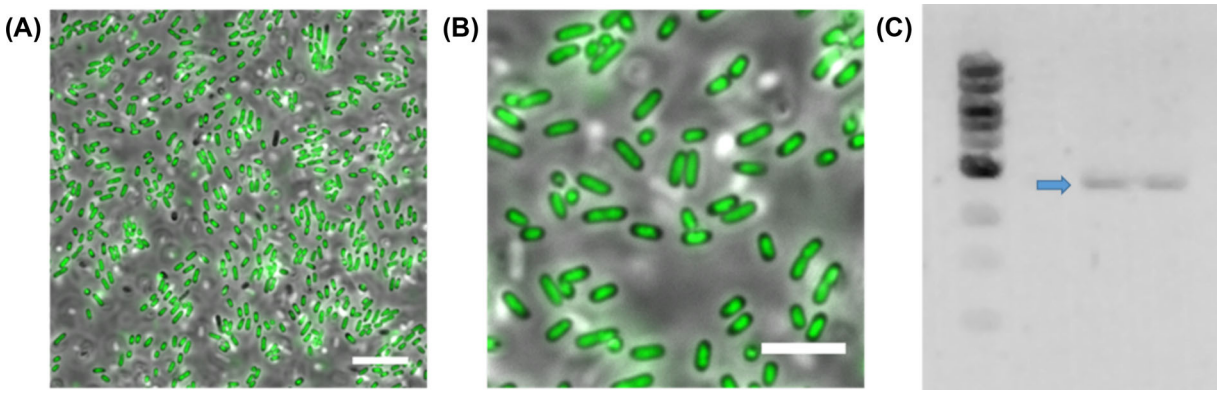

Figure 1. Chromosomal expression of HUα-GFP protein. (**A**) Composite phase contrast and a fluorescence image of recombinant cells from a colony demonstrate that the vast majority of cells express the fusion protein. (**B**) Enlarged fraction of image A demonstrating the localization of the fluorescence to nucleoids. (**C**) Colony PCR with appropriate primers showing the correct size (arrow, compare with the 1 kb DNA ladder (New England Biolabs Inc., Ipswich, MA) in the left line) and the location of the insert on the chromosome. The scale bar is 10 and 5 microns in images A and B, respectively.

Functional HU is a heterotypic dimer, HU$\alpha\beta$, or homodimers, HUα_2 and HUβ_2, composed of two closely related subunits encoded by the *hupA* and *hupB* genes, respectively (Dillon and Dorman 2010). In *Escherichia coli*, the *hupAB* double deletion has a mild effect, namely, it results in slow growth and a highly pleiotropic phenotype (Wada *et al.* 1988; Huisman *et al.* 1989; Kano and Imamoto 1990; Dri, Rouviere-Yaniv and Moreau 1991; Painbeni, Caroff and Rouviere-Yaniv 1997; Li and Waters 1998; Oberto *et al.* 2009). In contrast, in *Bacillus subtilis*, mutations in HU are lethal (Micka and Marahiel 1992; Fernandez, Rojo and Alonso 1997). Mutation and gene disruption analyses have validated the biological significance of HU across various species (Yasuzawa *et al.* 1992; Boubrik and Rouviere-Yaniv 1995; Liu *et al.* 2008). Interestingly, HU has been suggested as a potential target for the development of therapies against tuberculosis (Bhowmick *et al.* 2014). The HU subunit composition is a function of the physiological state of the cell (Claret and Rouviere-Yaniv 1997); specifically, the HU$\alpha\beta$ heterodimer is prevalent throughout the exponential phase, and the homodimers HUα_2 and HUβ_2 are specific for the lag and stationary phases, respectively. Moreover, the overall composition of DNA-binding proteins changes upon the cessation of active growth. Ali Azam *et al.* (1999) and Talukder and Ishihama (2015) showed that HU, Fis, H-NS, StpA and Hfq are dominant in exponentially growing cells, whereas Dps occupies more than half of the stationary phase nucleoid. Thus far, the content of HU at different exponential growth rates and during the cell cycle has not been well explored.

In this work, for the first time we quantified HU in *E. coli* cells at different growth rates as well as its dynamics during the cell cycle. The cellular content of HU was estimated using eGFP fusion under the native HUα promotor on the chromosome. We found that the cellular concentration of HUα increases with the cell growth rate, and its amount per genome equivalent is also remarkably higher.

MATERIALS AND METHODS

Construction of a strain containing the HU fluorescent reporter

To generate a strain carrying a single constitutive chromosomal copy of a fluorescent reporter, we inserted an *egfp* gene in frame immediately downstream of endogenous *hupA* in the MG1655 strain of *Escherichia coli*. This approach was successfully used to study the morphology dynamics of nucleoids visualized by chromosomally encoded HupA-mCherry (Fisher *et al.* 2013). Attachment of the reporter protein to the apparently less functional C-terminal of Huα (Ramstein *et al.* 2003) and choice of strictly monomeric eGFP are aimed to minimize possible interference with native interactions of the tagged protein. Cloning vector pEGFP (Clontech Laboratories, Inc., Palo Alto, CA) served as the source of *egfp*. In view of the possible susceptibility to H-NS-mediated silencing (Corcoran, Cameron and Dorman 2010), the gene sequence was analyzed for predicted curvature and appeared to be an unlikely target for H-NS. The chromosomal insertion of *egfp* was performed by recombineering (recombination-mediated genetic engineering) using pSIM5 plasmid (courtesy of Prof. Court's lab, National Cancer Institute in Frederick, MD, USA), following the methodology described in Thomason *et al.* (2014). pBAD24 plasmid containing *egfp* was used as a PCR template for amplifying the *egfp–ampR* cassette using the following primers: forward 5′-GTACCGGCATTTGTTTCTGGCAAGGCACTGAAAGACGCAGTTAAG TCTCGCATGGTGAGCAAGGGCGAGGAGCTG-3′ and reverse 5′-CCAGCCAGCATCAATGATCGACGCCAGAAAGACAAAAGGGGTGA AACCACCTGGCAAGTGTAGCGGTCACG-3′. The obtained 2.3 kb PCR product was inserted into MG1655 cells carrying pSIM5 plasmid according to the mentioned protocol (Thomason *et al.* 2014). The transformants were selected on LB plates supplemented with 40 μg/ml of ampicillin. The resulting colonies were screened for the nucleoid localization of fluorescence, and the insert localization was verified by colony PCR with the following primers: forward 5′-CGGTGCGTGTATGCAGGAGAGTGC-3′ and reverse 5′-CAGATGCACATTATCGCCGCTGTC-3′ (Fig. 1C).

Wild-type and HUα-eGFP strains were grown in LB and minimal M9 medium with various carbon sources. We found that the modified strain had exactly the same growth rate as that of the wild type, which validates that the fusion does not affect the normal physiology. In the recombinant cells, expression of this protein is expected to be at the native level and without any external induction. Microscopic examination clearly confirmed the nucleoid localization of fluorescence (Figs 1A, B and 2).

Growth conditions and sample preparation for microscopy

Escherichia coli MG1655-HUαGFP cells were grown at 37°C in LB medium (growth rate 2.50 h^{-1}) or in minimal M9 medium

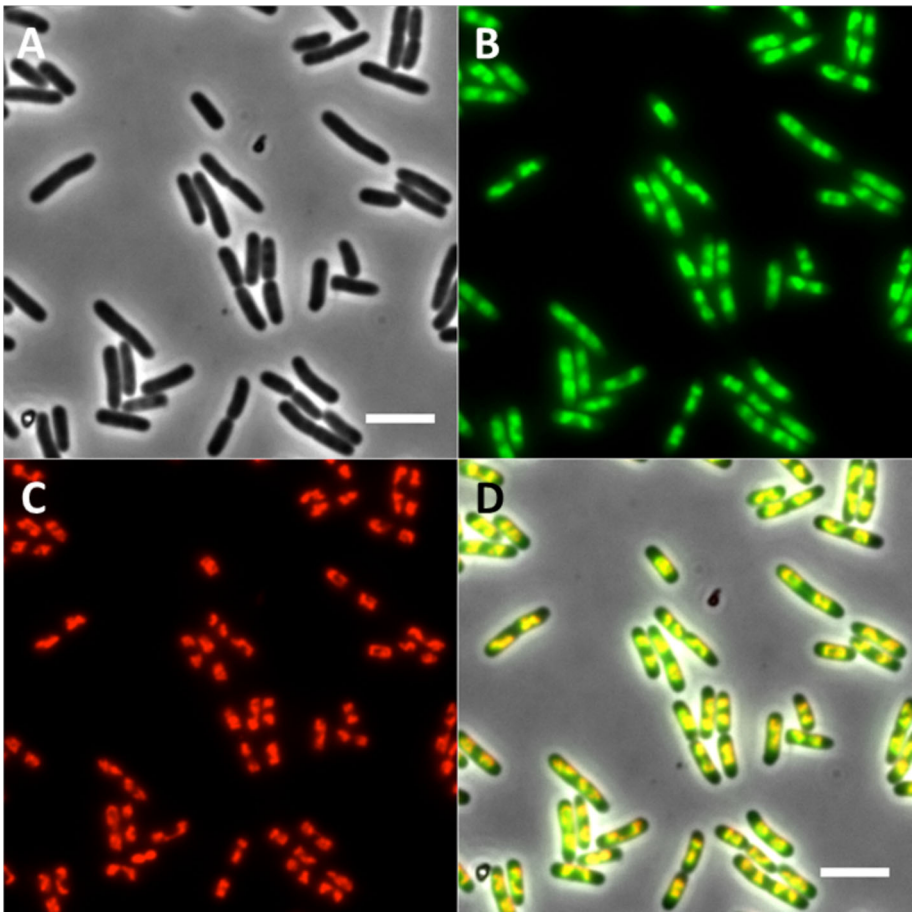

Figure 2. Chromosomally encoded HUα-GFP stains the nucleoid. Exponentially growing *E. coli* MG1655 cells (LB medium, 22 min generation time) were fixed with 1% formaldehyde, stained with DAPI and imaged on the agar pad using phase contrast (**A**), or GFP (**B**) and DAPI (**C**) fluorescence (with green and red LUTs applied, respectively). (**D**) Merged images A, B and C. Scale bar is 5 μm.

supplemented with different carbon sources: 0.2% glycerol and 1% tryptone (2.07 h^{-1}), 0.2% glucose (0.91 h^{-1}), 0.2% glycerol (0.56 h^{-1}) and 1μg/ml thiamine. All media contained 40 μg/ml ampicillin. Cells were grown exponentially for 8–10 generations to an optical density of 0.2 at 600 nm, at which point 200 μl of the culture was fixed with 0.25% paraformaldehyde for 15 min at room temperature and consequently stained with 2 μM 4′,6-diamidino-2-phenylindole (DAPI) for 30 min at 37°C. The fixation was aimed first to examine cells in a particular functional state (exponential), as well as to enable DAPI staining and, moreover, to ensure a complete maturation of the fluorescent protein. Four microliters of the stained cells were placed on a 2% agarose pad that was prepared on PBS.

For time-lapse experiments, an aliquot from the batch culture was mounted on the agarose pad prepared on the LB medium with preformed groves as described in Hadizadeh Yazdi *et al.* (2012). The sample chamber was maintained at 37°C.

Image acquisition and processing

Images were taken using a Zeiss Axiovert 200M fluorescence microscope equipped with a 100×/1.4 plan-apochromat objective, an AxioCam HRm camera, eGFP and DAPI filter sets and a temperature-controlled incubator. The microscope operation and image acquisition were controlled by the AxioVision SE (V4.9.1.0) program. A reduced light intensity (1D neutral filter in the excitation path) was used to minimize photobleaching of fluorophores. Optimal exposure times were chosen based on the determination of the linear range in mean ROI pixel intensity dependences on exposure time for both GFP and DAPI. This allowed achieving appropriate signal/background ratio and to avoid saturation. All images were acquired with the same corresponding exposure times and light power to enable us to correctly compare the intensities. In the time-lapse regime, the series of phase-contrast and fluorescence images were acquired with 1 min intervals for several generations at 37°C. Images were analyzed using ImageJ software (W. Rasband, http:// imagej.nih.gov/ij/). Phase-contrast images were used for thresholding, and the background of the fluorescence images was subtracted using the rolling ball (80-pixel radius) procedure of ImageJ. We used mean and integral density as measures of the concentration and the total amount of protein in cells, respectively. For visual presentation, images were processed using enhance contrast routine of ImageJ.

RESULTS AND DISCUSSION

Fluorescence of chromosomally encoded *hupA-egfp* quantitatively reveals the amount of DNA in the *Escherichia coli* MG1655 population

The reliability of nucleoid staining with chromosomally encoded HUα-GFP was verified by comparing the GFP fluorescence intensity and localization from exponentially growing cells with

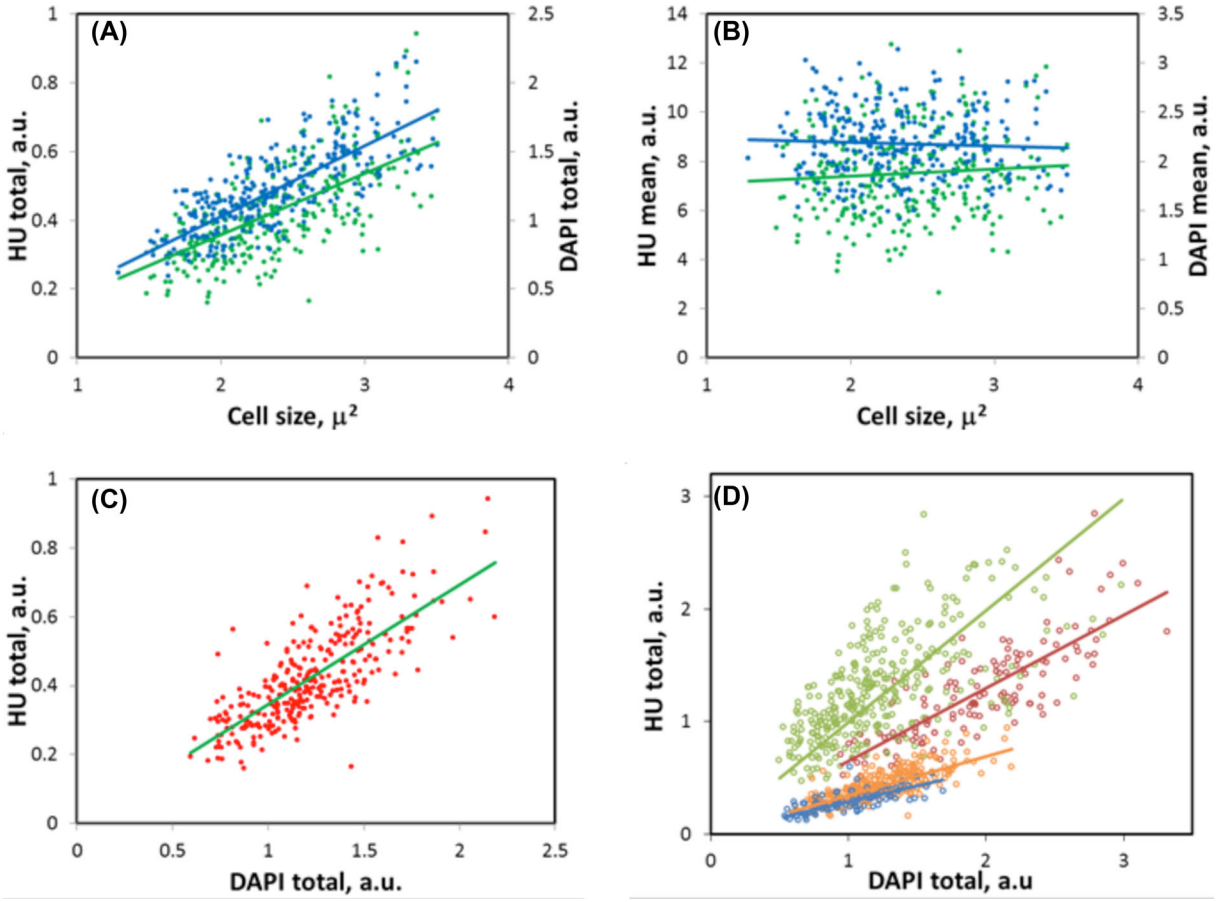

Figure 3. The amount of HUα linearly correlates with the cell size and the DNA content in a population of cells. Total (**A**) and mean (**B**) amount of HUα-GFP (green dots) and DAPI (blue dots) fluorescence intensity from individual cells as a function of the cell size. More than 300 cells were measured in a fixed steady-state culture grown in M9 medium with glucose (generation time 64 min). Cell size is expressed as the cell area in phase contrast images. (**C**) Correlation between HUα and DAPI fluorescence intensities. Lines represent linear fits of the data. (**D**) Same as C, but for all growth media tested: LB (red), M9 supplemented with 0.2% glycerol and 1% tryptone (green), 0.2% glucose (orange) and 0.2% glycerol (blue). Each dot in the plots represents a single cell.

those of the DNA-specific stain DAPI (Kapuscinski 1995). The correlation between the fluorescence from the two staining techniques was demonstrated both at the single-cell level (Fig. 2) and in a sample of the population (Fig. 3). GFP fluorescence was well co-localized with DAPI fluorescence in steady-state growing cells (Fig. 2), indicating that most of the HUα protein is DNA bound. Indeed, only about 6% of HUα were estimated as cytoplasmic (Pelletier *et al.* 2012). Note that formaldehyde treatment was used, first, to fix a specific physiological state of bacteria, avoiding possible changes in the HUα concentration during the sample preparation and microscopy and, second, to facilitate DAPI staining because live cells are weakly permeable to this dye. Moreover, the additional incubation time needed for fixation and staining allows complete fluorophore maturation of the existing GFP, thus providing an estimation of the actual amount of HU in bacteria. Comparing the HUα-GFP images of fixed and live cells (see Figs 2 and 5), we noted a less pronounced localization of the fluorescence to the nucleoid and a remarkable amount of it in the cytoplasm of the fixed cells. This was not caused by cleavage or degradation of the fused protein, as examined by fluorescence imaging of the total cell protein SDS-PAGE (data not shown). Most probably, the formaldehyde modification of HUα weakens its binding affinity to DNA, causing partial dissociation from the nucleoid. However, this dissociation does not influence how the amount of HUα in a cell can be correctly estimated, since the thresholding method based on the phase-contrast images reveals all the intracellular fluorescence, independently of its localization (see Methods for details).

The fact that in our recombinant strain all of the HUα proteins are labeled with the fused GFP enabled us to quantitatively estimate the HUα amount and concentration in these cells using digital processing of microscopic images. In addition, we applied DAPI staining of fixed cells to correlate HUα content with that of DNA, assuming that the DAPI fluorescence intensity reflects the amount of DNA (Kapuscinski 1995). This approach obviously requires standardization of the whole procedure, ranging from staining to image acquisition, processing and analysis. The integral cellular fluorescence intensities therefore correspond to the total protein and DNA content per cell, and the mean cellular intensity (per pixel) corresponds to their concentration. Our results indicate that the amounts of HUα and DNA are linearly correlated with the cell size (Fig. 3A), with a correlation coefficient of about 0.8–0.9 for different experiments and a standard relative deviation from the linear regression of about 12%–14%. In general, cell size in a steady-state growing culture correlates with the cell age in the division cycle, although an essential individual variability is usually observed in the growth rates and cell sizes (Reshes *et al.* 2008a). This variability is responsible for the observed dispersion of the data (Fig. 3) because the cells of the same size do not necessarily belong to the same age and

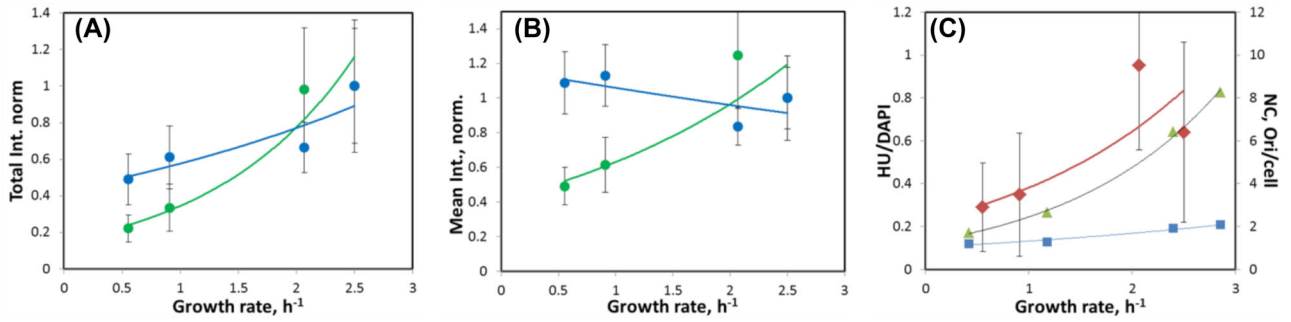

Figure 4. HUα and DNA content in cells growing at different rates. Integral ('Total,' **A**) and mean (**B**) fluorescence intensity was measured in a set of cells (>300) from cultures grown to steady-state in different media as described in Methods. For uniformity, all cultures were grown in parallel; samples were taken at the evident steady-state growth of each culture, fixed with formaldehyde, stained with DAPI and prepared for microscopy on agarose pads. Images were acquired under the same conditions of illumination, exposure and temperature. The average population values ± SD of GFP (green) and DAPI (blue) fluorescence intensities in A and B were normalized to the highest growth rate; the values of HUα/DAPI ratio (**C**, red) were calculated as slopes of the linear fits for HUα vs DAPI (Fig. 3C) for each population. For a comparison, the nucleoid complexity values (blue) and the number of oriC/cell (green) for the same range of growth rates are shown in panel C. Results from one experiment are shown from a series of five, all reproducing the same trend of HUα/DAPI dependence on the growth rate. The lines are exponential fits to the data according to the generalized equations for macromolecular composition (Bremer and Dennis 2008). Nucleoid complexity and the number of oriC/cell were calculated using data for the C and D periods in *E. coli* MG1655 taken from Stokke, Flatten and Skarstad (2012) according to equations 3, 7 and 8 in Bremer and Dennis (2008).

therefore may contain different amounts of a particular protein. Hence, it can be concluded that the cellular amount of HUα gradually increases during the cell cycle at the same rate as the cell size, thus maintaining a constant concentration (Fig. 3B). The resulting linear correlation between HUα and the DNA cellular content (Fig. 3C) is a manifestation of a constant HUα/DNA ratio of this structure maintenance protein. This may reflect the existence of an auto-regulation mechanism underlying the HUα cellular level (Kohno *et al.* 1990; Kohno *et al.* 1994), beyond the duplication of the gene copy number during the cell cycle.

HUα content in *Escherichia coli* cells at different growth rates

In addition, we examined the HUα cellular content in the strain *E. coli* MG1655-HUGFP grown in media of various compositions, supporting the growth rates as specified in Methods. Very similar population dependences of HUα content were observed for all growth rates (Fig. 3D). As expected, there is a higher amount of DNA in faster growing cells (Bremer and Dennis 2008) and, correspondingly, a higher HUα content (Fig. 4A). However, the concentrations of HUα and DNA change inversely as the growth rate increases, whereas the DNA concentration slightly decreases (the average cell size increases to a greater extent than does the DNA content), and the HUα concentration nearly doubles (Fig. 4B). Accordingly, the ratio of HUα to DNA in cells strongly increases with the growth rate (Fig. 4C). Although the distribution of this ratio in a population is remarkably wide, as shown by the SD bars in Fig. 4C, the difference in the mean values is about 3-fold between growth rates of 0.5 and 2.5 h^{-1} and is statistically significant ($P < 0.001$). It was previously demonstrated that the cellular amount of HUα drops dramatically, about to the same extent, during the transition from the exponential to stationary phases (Ali Azam *et al.* 1999), along with the essential changes in the overall protein composition of the nucleoid (Talukder and Ishihama 2015). These changes were ascribed to the transformation of a functionally active nucleoid to a more compacted, protected morphology. To understand the growth rate-dependent variation in HUα/DNA stoichiometry in exponential cells observed by us, one needs to consider the differences in the nucleoid's functional and structural states at different growth rates.

In bacteria, faster growth rates (in particular, when the cell cycle is shorter than the sum of the replication (C) and septation (D) periods) imply a deeper overlap of the consequent chromosome replication cycles, leading to increased nucleoid complexity (Zaritsky, Wang and Vischer 2011; Zaritsky 2015). Thus, higher HUα/DNA stoichiometry may indicate a greater demand for maintaining the chromosome structure in nucleoids with higher complexity in faster growing cells. Nucleoid complexity is expressed as the ratio of the average DNA/cell value to the number of termini (Zaritsky 2015). However, the calculated nucleoid complexity value changes remarkably less than HUα/DNA in the same range of growth rates (Fig. 4C). Another manifestation of the overlapping replication cycles is the average number of origins of replication (oriC) per cell. It can be seen from Fig. 4C that HUα/DNA increases in parallel to the number of oriC/cell with increasing growth rates, indicative of its possible role in maintaining an extended structure of the highly branched chromosome. Moreover, it might reflect the important role of HU in the DNA replication process, at both the initiation and elongation steps (Bahloul, Boubrik and Rouviere-Yaniv 2001). In support of this notion, single-molecule studies have demonstrated an inversion of the compacting effect of low HU concentrations on the stabilization of a rigid extended, looped DNA conformation above the threshold concentration of the protein (van Noort *et al.* 2004; Stavans and Oppenheim 2006). In addition, in slow-growing bacteria, as happens during starvation or at the onset of the stationary phase of growth in batch cultures, there is less transcriptional activity and a corresponding relaxation in the looped domain structure of the nucleoid (Dillon and Dorman 2010). Fast-growing bacteria are more transcriptionally active, especially at genes coding for ribosome components and other parts of the translation machinery, and have more looped DNA domains. The higher HUα/DNA ratio may be required to stabilize these loops and the accompanying higher supercoiling density (Higgins 2014).

The increasing HUα/DNA ratio can be partially explained by a higher copy number of *hup* genes in faster growing cells relative to DNA content, just based on their proximity to oriC (Kano *et al.* 1985; Kano *et al.* 1987). However, negative auto-regulation of the *hupA* expression (Kohno *et al.* 1990; Kohno *et al.* 1994) could compensate for the increased gene copy number, and other regulatory circuits may also be involved (Claret and Rouviere-Yaniv 1996). Expression and synthesis of HU proteins are evidently regulated according to the physiological state of bacteria, at least at different growth stages (Claret and Rouviere-Yaniv 1997).

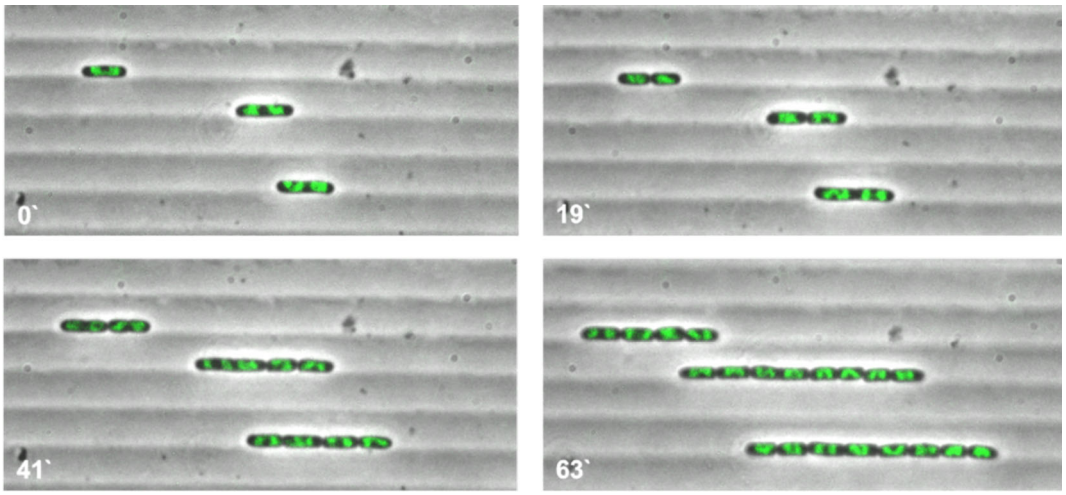

Figure 5. *Escherichia coli* MG1655-HUGFP cells growing in an agarose gel microchannel. Cells from exponentially grown batch culture (LB medium, 23.5 min generation time) were mounted on an agarose gel pad with imprinted microchannels, and phase contrast and fluorescence images were acquired in a time-lapse regime (1 min intervals) as described in Methods. Shown are overlaid consecutive phase contrast and fluorescence (HUα-GFP) images at times approximately corresponding to the division times. The average length doubling time of all lineages was 24.4 min. Background subtraction of the fluorescence images was performed as indicated in Methods.

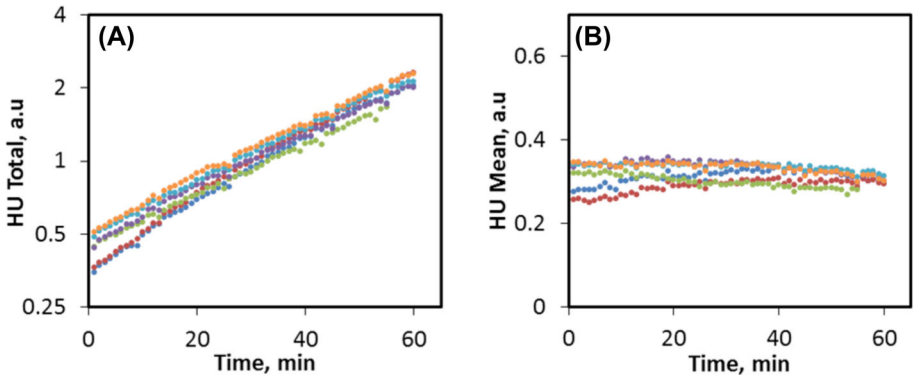

Figure 6. Single-cell analysis of HUα content. Time-lapse images of the lineages of six cells in the same field were acquired with a 1 min interval during the time shown and analyzed for integral (**A**) and mean (**B**) GFP fluorescence intensity, reflecting the dynamics of the HUα amount and concentration, respectively. The exposure time was 50 msec and 500 msec for the phase contrast and fluorescence channels, respectively. The results were reproduced well in a number of independent experiments.

However, the mechanism underlying this regulation and its role remains unclear. Taking into consideration the pleiotropic effect of HU on a wide number of the chromosome-related activities and on a wide range of the nucleoid structural levels (Hammel *et al.* 2016), more experimentation will be required to better understand the role and regulation of HU/DNA stoichiometry.

Single-cell cycle dynamics of HUα

As noted before, the cell length in a steady-state growing bacterial population may be used as a means of estimating the cell age in the division cycle. However, the native variability in growth rates and the sizes of individual cells hinder the possible cell cycle dynamics of a protein or event in the population analysis (Reshes *et al.* 2008b). Therefore, these dynamics were studied in more detail using single-cell live microscopy imaging. After the cells were grown in LB batch culture for several generations, steady-state cells were transferred to agarose gel pads prepared on a desired growth medium in order to follow single cells over several generations under constant environmental conditions (nutrient composition and temperature). Alignment of cells in preformed microchannels allows convenient imaging of individual cell lineages. An example of such lineages is presented in Fig. 5. The average doubling time of the lineage length on an agarose pad (24.4 min) was practically the same as the generation time of the corresponding batch culture (23.5 min).

The amount of HUα in all lineages exponentially increased with time for at least three cell cycles (Fig. 6A), whereas the HUα concentration in a single cell was maintained nearly constant (Fig. 6B). Although the total amount of HUα per lineage is measured, we can conclude that there are no significant changes in the rate of HUα synthesis and its concentration during the cell cycle because the second and third divisions in a lineage are well synchronized. The slight variation in concentrations among lineages presumably reflects the variability of HUα content in individual primary cells. These results are generally consistent with those obtained from population studies (the independence of the average HUα concentration on the cell size; Fig. 3B). The constant HUα concentration during the cell cycle may indicate an overwhelming effect of autoregulation on *hupA* expression (Kohno *et al.* 1990; Kohno *et al.* 1994) despite the doubling of the gene copy number during the replication cycle.

CONCLUSIONS

The presented data suggest that the concentration of HUα in exponentially growing *Escherichia coli* cells is maintained constant throughout the cell cycle. This concentration increases in faster growing cells, resulting in a higher HUα/DNA stoichiometry. The latter phenomenon, observed here for the first time, may indicate that different regulatory mechanisms are involved in maintaining the functional morphology of nucleoids with varying complexity. Considering the multiplicity of the relevant regulatory pathways and the pleiotropic effects of HU, further comprehensive studies are required to decipher the HU-nucleoid relationships.

ACKNOWLEDGEMENTS

We are most grateful to Prof. D. L. Court, National Cancer Institute in Frederick, MD, USA, for his generous gift of pSIM5 plasmid for our recombineering work. The highly professional help of Mrs. Sonia Soreanu was indispensable.

FUNDING

This work was performed with financial support from the Israel Science Foundation (ISF grant no. 1701/13 to IF) and in part from the German–Israeli Foundation for Scientific Research and Development (GIF grant no. 1160-137.14/2011 to IF). AA's salary was covered in part by the Returning Scientist support program of the Israeli Ministry of Immigrant Absorption, and AHA received part of his stipend from the Kreitman School of Advanced Graduate Studies at Ben-Gurion University, Israel.

Conflicts of interest. None declared.

REFERENCES

Aki T, Adhya S. Repressor induced site-specific binding of HU for transcriptional regulation. *EMBO J* 1997;**16**:3666–74.

Ali Azam T, Iwata A, Nishimura A *et al.* Growth phase-dependent variation in protein composition of the *Escherichia coli* nucleoid. *J Bacteriol* 1999;**181**:6361–70.

Bahloul A, Boubrik F, Rouviere-Yaniv J. Roles of *Escherichia coli* histone-like protein HU in DNA replication: HU-beta suppresses the thermosensitivity of dnaA46ts. *Biochimie* 2001;**83**:219–29.

Becker NA, Kahn JD, Maher LJ. Eukaryotic HMGB proteins as replacements for HU in *E-coli* repression loop formation. *Nucleic Acids Res* 2008;**36**:4009–21.

Berger M, Farcas A, Geertz M *et al.* Coordination of genomic structure and transcription by the main bacterial nucleoid-associated protein HU. *EMBO Rep* 2010;**11**:59–64.

Bhowmick T, Ghosh S, Dixit K *et al.* Targeting *Mycobacterium tuberculosis* nucleoid-associated protein HU with structure-based inhibitors. *Nat Commun* 2014;**5**:4124.

Boubrik F, Rouviere-Yaniv J. Increased sensitivity to gamma irradiation in bacteria lacking protein HU. *Proc Natl Acad Sci U S A* 1995;**92**:3958–62.

Bremer H, Dennis P. Modulation of chemical composition and other parameters of the cell at different exponential growth rates. *EcoSal Plus* 2008, DOI: 10.1128/ecosal.5.2.3.

Broyles SS, Pettijohn DE. Interaction of the *Escherichia-coli* Hu protein with DNA - evidence for formation of nucleosome-like structures with altered DNA helical pitch. *J Mol Biol* 1986;**187**:47–60.

Chodavarapu S, Felczak MM, Yaniv JR *et al.* *Escherichia coli* DnaA interacts with HU in initiation at the *E. coli* replication origin. *Mol Microbiol* 2008;**67**:781–92.

Claret L, Rouviere-Yaniv J. Regulation of HU alpha and HU beta by CRP and FIS in *Escherichia coli*. *J Mol Biol* 1996;**263**:126–39.

Claret L, Rouviere-Yaniv J. Variation in HU composition during growth of *Escherichia coli*: the heterodimer is required for long term survival. *J Mol Biol* 1997;**273**:93–104.

Corcoran CP, Cameron AD, Dorman CJ. H-NS silences gfp, the green fluorescent protein gene: gfpTCD is a genetically remastered gfp gene with reduced susceptibility to H-NS-mediated transcription silencing and with enhanced translation. *J Bacteriol* 2010;**192**:4790–3.

Dame RT, Goosen N. HU: promoting or counteracting DNA compaction? *FEBS Lett* 2002;**529**:151–6.

Dillon SC, Dorman CJ. Bacterial nucleoid-associated proteins, nucleoid structure and gene expression. *Nat Rev Microbiol* 2010;**8**:185–95.

Dorman CJ, Deighan P. Regulation of gene expression by histone-like proteins in bacteria. *Curr Opin Genet Dev* 2003;**13**:179–84.

Dri AM, Rouviere-Yaniv J, Moreau PL. Inhibition of cell division in hupA hupB mutant bacteria lacking HU protein. *J Bacteriol* 1991;**173**:2852–63.

Fernandez S, Rojo F, Alonso JC. The *Bacillus subtilis* chromatin-associated protein Hbsu is involved in DNA repair and recombination. *Mol Microbiol* 1997;**23**:1169–79.

Fisher JK, Bourniquel A, Witz G *et al.* Four-dimensional imaging of *E. coli* nucleoid organization and dynamics in living cells. *Cell* 2013;**153**:882–95.

Hadizadeh Yazdi N, Guet CC, Johnson RC *et al.* Variation of the folding and dynamics of the *Escherichia coli* chromosome with growth conditions. *Mol Microbiol* 2012;**86**:1318–33.

Hammel M, Amlanjyoti D, Reyes FE *et al.* HU multimerization shift controls nucleoid compaction. *Sci Adv* 2016;**2**:e1600650.

Higgins NP. RNA polymerase: chromosome domain boundary maker and regulator of supercoil density. *Curr Opin Microbiol* 2014;**22**:138–43.

Hodges-Garcia Y, Hagerman PJ, Pettijohn DE. DNA ring closure mediated by protein HU. *J Biol Chem* 1989;**264**:14621–3.

Huisman O, Faelen M, Girard D *et al.* Multiple defects in *Escherichia coli* mutants lacking HU protein. *J Bacteriol* 1989;**171**:3704–12.

Kamashev D, Rouviere-Yaniv J. The histone-like protein HU binds specifically to DNA recombination and repair intermediates. *EMBO J* 2000;**19**:6527–35.

Kano Y, Imamoto F. Requirement of integration host factor (IHF) for growth of *Escherichia coli* deficient in HU protein. *Gene* 1990;**89**:133–7.

Kano Y, Osato K, Wada M *et al.* Cloning and sequencing of the HU-2 gene of *Escherichia coli*. *Mol Gen Genet* 1987;**209**:408–10.

Kano Y, Yoshino S, Wada M *et al.* Molecular cloning and nucleotide sequence of the HU-1 gene of *Escherichia coli*. *Mol Gen Genet* 1985;**201**:360–2.

Kapuscinski J. DAPI: a DNA-specific fluorescent probe. *Biotech Histochem* 1995;**70**:220–33.

Kohno K, Wada M, Kano Y *et al.* Promoters and autogenous control of the *Escherichia coli* hupA and hupB genes. *J Mol Biol* 1990;**213**:27–36.

Kohno K, Yasuzawa K, Hirose M *et al.* Autoregulation of transcription of the hupA gene in *Escherichia coli*: evidence for steric

hindrance of the functional promoter domains induced by HU. *J Biochem* 1994;**115**:1113–8.

Li SS, Waters R. *Escherichia coli* strains lacking protein HU are UV sensitive due to a role for HU in homologous recombination. *J Bacteriol* 1998;**180**:3750–6.

Liu D, Yumoto H, Murakami K *et al*. The essentiality and involvement of *Streptococcus intermedius* histone-like DNA-binding protein in bacterial viability and normal growth. *Mol Microbiol* 2008;**68**:1268–82.

Micka B, Marahiel MA. The DNA-binding protein Hbsu is essential for normal growth and development in *Bacillus-subtilis*. *Biochimie* 1992;**74**:641–50.

Oberto J, Nabti S, Jooste V *et al*. The HU regulon is composed of genes responding to anaerobiosis, acid stress, high osmolarity and SOS induction. *PLoS One* 2009;**4**:e4367.

Painbeni E, Caroff M, Rouviere-Yaniv J. Alterations of the outer membrane composition in *Escherichia coli* lacking the histone-like protein HU. *Proc Natl Acad Sci U S A* 1997;**94**:6712–7.

Pelletier J, Halvorsen K, Ha BY *et al*. Physical manipulation of the *Escherichia coli* chromosome reveals its soft nature. *Proc Natl Acad Sci U S A* 2012;**109**:E2649–56.

Ramstein J, Hervouet N, Coste F *et al*. Evidence of a thermal unfolding dimeric intermediate for the *Escherichia coli* histone-like HU proteins: thermodynamics and structure. *J Mol Biol* 2003;**331**:101–21.

Reshes G, Vanounou S, Fishov I *et al*. Cell shape dynamics in *Escherichia coli*. *Biophys J* 2008a;**94**:251–64.

Reshes G, Vanounou S, Fishov I *et al*. Timing the start of division in *E. coli*: a single-cell study. *Phys Biol* 2008b;**5**:046001.

Stavans J, Oppenheim A. DNA-protein interactions and bacterial chromosome architecture. *Phys Biol* 2006;**3**:R1–10.

Stokke C, Flatten I, Skarstad K. An easy-to-use simulation program demonstrates variations in bacterial cell cycle parameters depending on medium and temperature. *PLoS One* 2012;**7**:e30981.

Talukder A, Ishihama A. Growth phase dependent changes in the structure and protein composition of nucleoid in *Escherichia coli*. *Sci China Life Sci* 2015;**58**:902–11.

Thomason LC, Sawitzke JA, Li X *et al*. Recombineering: genetic engineering in bacteria using homologous recombination. *Curr Protoc Mol Biol* 2014;**106:V:1.16**:1.16.1–1.16.39.

van Noort J, Verbrugge S, Goosen N *et al*, Dual architectural roles of HU: formation of flexible hinges and rigid filaments. *Proc Natl Acad Sci U S A* 2004;**101**:6969–74.

Wada M, Kano Y, Ogawa T *et al*. Construction and characterization of the deletion mutant of hupA and hupB genes in *Escherichia coli*. *J Mol Biol* 1988;**204**:581–91.

Wei J, Czapla L, Grosner MA *et al*. DNA topology confers sequence specificity to nonspecific architectural proteins. *Proc Natl Acad Sci U S A* 2014;**111**:16742–7.

Yasuzawa K, Hayashi N, Goshima N *et al*. Histone-like proteins are required for cell growth and constraint of supercoils in DNA. *Gene* 1992;**122**:9–15.

Zaritsky A. Cell-shape homeostasis in *Escherichia coli* is driven by growth, division, and nucleoid complexity. *Biophys J* 2015;**109**:178–81.

Zaritsky A, Wang P, Vischer NO. Instructive simulation of the bacterial cell division cycle. *Microbiology* 2011;**157**:1876–85.